AIAA AVIATION Forum
17-21 June 2019, Dallas, Texas
AIAA Aviation 2019 Forum

10.2514/6.2019-3041

Modeling of Brown-Michael vortices in ground effect

Huansheng Chen*
Lehigh University, Bethlehem, Pennsylvania, 18015

Peter J. Baddoo †
University of Cambridge, Cambridge, CB3 0WA, United Kingdom

Justin W. Jaworski‡
Lehigh University, Bethlehem, Pennsylvania, 18015

Biological fliers and swimmers often operate in proximity to a wall or ground plane to improve their lift-to-drag ratio. However, unsteady aerodynamics models that are restricted to single objects are unable to account for this so-called ground effect. In this paper, a analytic reduced-order vortex model is developed for a flat plate in ground effect. The complex potential is calculated in an annular domain, which is mapped to the physical domain via a conformal mapping that employs the transcendental Schottky-Klein prime function. The effects of vortex shedding are modelled with the Brown-Michael equation.

I. Introduction

Natural fliers commonly utilise a ground plane to enhance their lift-to-drag ratio [1]. Vehicle designers [2–4] also seek to exploit this "ground effect" phenomenon, and consequently the accurate mathematical modelling of the flow field is required. Such a model must be physically accurate and computationally efficient if it is to be used in any optimisation loop for vehicle design. However, current vortex models [5, 6] are restricted to single-body interactions and cannot take into account the effect of a ground plane. There are both numerical [7–9] and asymptotic [10–12] investigations, but this paper proposes a vortex model that is swift to compute and is not restricted to an asymptotic regime where the body is either very close or far away from the planar wall.

Two-dimensional unsteady flow with low Mach number and high Reynolds number past an airfoil is a classical problem in fluid-structure interactions that has received considerable attention in the aeronautical literature over the past century. For theoretical analyses in particular, the representation of how vorticity is shed into the wake to satisfy the Kutta condition at the trailing edge plays a crucial role in gust-airfoil interactions and related unsteady airfoil problems. An early model to account for the effect of vortex shedding of a delta wing was formulated by Brown and Michael [13]. Their model supposes that the vorticity shed from an edge rolls up via a connecting vortex sheet into a point vortex with time-varying circulation. We refer to such vortices as Brown-Michael vortices, whose circulation is set instantaneously to satisfy the Kutta condition. The Brown and Michael equation describes the motion of the vortex tethered to the trailing edge before it is released as a free vortex into the flow. However, the original formulation does not guarantee the vanishing of a reaction force due to an unbalanced couple, which is of minor concern to the fluid dynamic problem but is important for aeroacoustic predictions based on the model. Howe [14] provided an emended version of the Brown-Michael equation which does not result in an unbalanced couple.

In the present work, the analyses of [15] and [16] are extended to include the influence of a ground plane. Advances in conformal mapping theory [17, 18] allow the complex potential to be expressed in terms of the Schottky-Klein prime function, which may be rapidly computed using a recently developed algorithm [19]. Adapting the approach of Baddoo and Ayton [20] allows the complex potential to be constructed and applied as a forcing for shed Brown-Michael vortices. The results of insight into the influence of a ground plane on lift production and aerodynamic performance.

*Ph.D. Student, Department of Mechanical Engineering and Mechanics, Student Member AIAA
†Ph.D. Candidate, Department of Applied Mathematics and Theoretical Physics, Student Member AIAA
‡Assistant Professor, Department of Mechanical Engineering and Mechanics, Senior Member AIAA

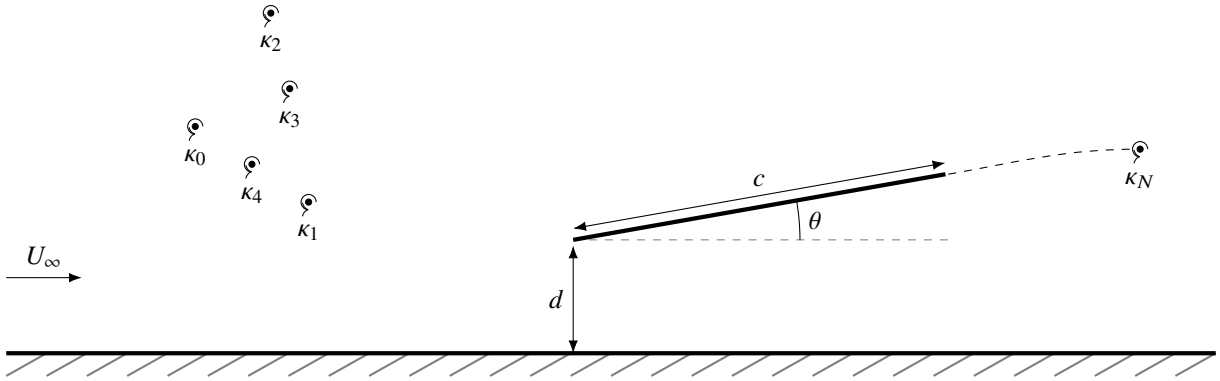

Fig. 1 A flat plate in ground effect with labelled length-scales. The chord length is $c = 1$, pitching angle θ, and ground proximity d. The origin is placed on the ground in-line with the trailing edge, while x is the streamwise direction and y is the lateral direction. Point vortices of strengths κ_j are labelled with spirals, and the dashed line indicates a branch cut connecting the trailing edge to the Brown-Michael vortex.

II. Mathematical formulation

Our analysis follows the work of [20] and is restricted to inviscid, irrotational, incompressible, two-dimensional flow. Therefore, there exists a complex potential function

$$w(z) = \phi(z) + \mathrm{i}\psi(z),$$

where ϕ and ψ are the velocity potential and stream function in the physical z-plane, respectively. Similarly to [20], we consider a plate of length c, inclined at angle θ to the ground, where the distance from the leading edge to the ground is d, as illustrated in figure 1. Far upstream and downstream, the flow is tangential to the ground and has speed U_∞. The fluid domain may contain a number of free and attached point vortices, which represent incident vorticity on the flat plate, its vorticity shed into the wake, and the Brown-Michael vortex shed from the trailing edge. No-flux boundary conditions are imposed on the ground and plate. Additionally, we specify the Kutta condition of finite flow velocity at the trailing edge. We non-dimensionalise length by c and velocity by U_∞.

A. Conformal map

Unlike the simple case of a single aerofoil [16], our domain is doubly-connected and therefore the traditional methods of conformal mappings to the unit disk or upper half-plane are not applicable. Consequently, we appeal to a similar conformal map as that used in the study of vortex equilibria in ground effect [20].

Since our domain is doubly-connected, the canonical circular domain is an annulus. We label the exterior circle of the annulus C_0 and the interior circle C_1, as illustrated in figure 2. The radius of the interior circle is given by q, which we vary to change the height from the ground, d. The conformal map we use is called the “radial slit map" [18], which depends on two parameters, and maps circular regions in the ζ-plane to slits pointing to a particular point in the z-plane. However, if one of the parameters is taken to lie C_0, the radial slit map becomes a radial half-plane map and C_0 is mapped to an infinite line. Furthermore, we may choose the second parameter in the radial slit map such that the (finite) image of C_1 is inclined at angle θ to the ground. The corresponding map is given as [20]

$$z = f(\zeta) = A\frac{\omega(\zeta, \mathrm{e}^{2\mathrm{i}\theta})}{\omega(\zeta, 1)} + s, \tag{1}$$

where A is a constant required to scale the plate to unit length and s is a constant that moves the plate so that the leading edge is above the origin. Both of these may be determined numerically using a simple Newton method. The Schottky-Klein prime function is denoted by $\omega(\cdot, \cdot)$.

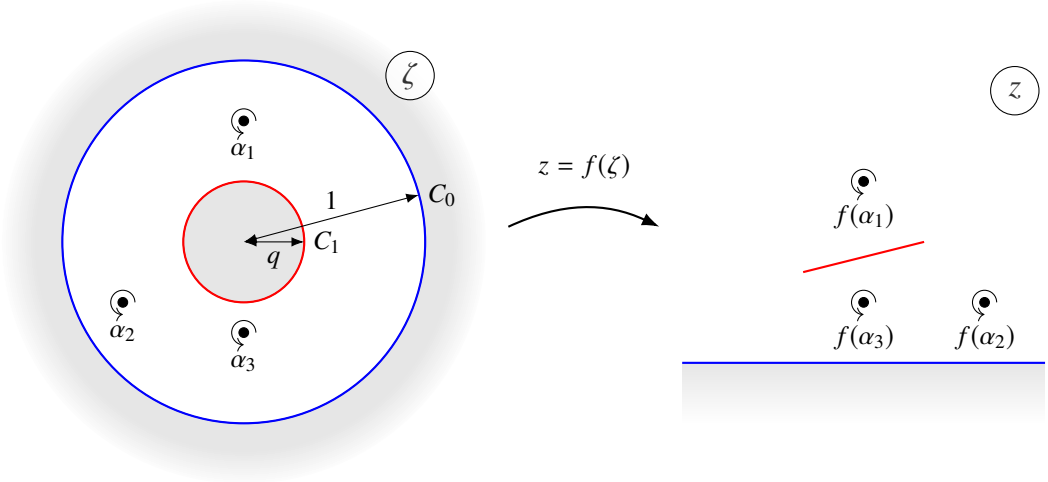

Fig. 2 Illustration of the conformal map from the transform ζ-space to the physical z-space. The inner red circle is mapped to the flat plate and the outer blue circle is mapped to the ground plane. The gray areas indicate regions that are outside the domain of definition. The point vortices with strengths κ_j located at α_j in the ζ-plane map to the z-plane, where the vortex strengths are preserved under the conformal mapping.

The Schottky-Klein prime function for the annulus can be expressed in two rapidly convergent forms [19, 21, 22]:

$$\omega(\zeta,\gamma) = \frac{\zeta-\alpha}{C^2}\prod_{k=1}^{\infty}\left(1-q^{2k}\frac{\zeta}{\alpha}\right)\cdot\left(1-q^{2k}\frac{\alpha}{\zeta}\right) \tag{2}$$

$$= -\frac{\alpha}{C^2}A\sum_{n=-\infty}^{\infty}(-1)^n q^{n(n-1)}\left(\frac{\zeta}{\alpha}\right)^n, \tag{3}$$

where

$$C = \prod_{k=1}^{\infty}\left(1-q^{2k}\right), \qquad A = \frac{\prod_{n=1}^{\infty}\left(1+q^{2n}\right)^2}{\sum_{n=1}^{\infty}q^{n(n-1)}}.$$

B. Complex potential

Since we have a conformal map from the annular domain to the physical domain, it is sufficient to calculate the complex potential in the annular domain. We appeal to the new calculus of vortex dynamics proposed by Crowdy [21], which provides a framework for the calculation of instantaneous complex potentials associated with multiply-connected domains. An advantage of this approach which we will exploit is its ability to specify the circulations around individual bodies.

We follow the procedures of [16] and [20], where the complex potential is split into three contributions: the contribution from the incident vortex W_Γ, the contribution from the shedding vortices W_κ, and the contribution from the uniform flow W_U.

1. Contribution from the incident vortex: $W_\Gamma(\zeta)$

Due to [21], we know that the hydrodynamic Green's function,

$$G^{(0)}(\zeta,\alpha) = \frac{1}{2\pi\mathrm{i}}\log\left(\frac{\omega(\zeta,\alpha)}{|\alpha|\omega(\zeta,1/\overline{\alpha})}\right), \tag{4a}$$

is the complex potential for a unit circulation point vortex at α in any canonical circular domain. An overbar denotes the complex conjugate. The hydrodynamic Green's function produces circulation -1 around the object which is the image of

C_0 and zero circulation around the other objects. To specify a non-zero circulation around the obstacle whose boundary is the image of C_1, we use the Möbius map $\theta_1(\zeta) = q^2\zeta$ and write the *modified* hydrodynamics Green's function

$$G^{(1)}(\zeta, \alpha) = \frac{1}{2\pi \mathrm{i}} \log\left(\frac{\omega(\zeta, \alpha)}{|\alpha|\omega(\zeta, \theta_1(1/\overline{\alpha}))}\right). \tag{4b}$$

The above corresponds to a point vortex of unit circulation at α but now has circulation -1 around the obstacle whose boundary is the image of C_1, i.e. the flat plate. Additionally, the modified hydrodynamics Green's function produces zero circulation around all other obstacles.

We are free to choose either Eq. (4a) or Eq. (4b) to represent the complex potential due to the vortices. However, since we wish the cancel the contributions to the circulation around any body, we are required to choose Eq. (4b). In order to cancel out the circulation around all bodies we must place a sufficiently strong vortex at the pre-image of infinity. The pre-image of infinity is $\zeta_\infty = 1$ and lies on the body C_0. Substituting $\alpha = \zeta_\infty$ into Eq. (4a) results in a constant, so we choose Eq. (4b) to represent the complex potential induced by a point vortex in the flow.

Therefore, the complex potential induced by the incident vortex of strength Γ at α_Γ, and produces no circulation around the plate C_1 is

$$\begin{aligned} W_\Gamma(\zeta) &= \Gamma G^{(1)}(\zeta, \alpha_\Gamma) - \Gamma G^{(1)}(\zeta, 1) \\ &= \frac{\Gamma}{2\pi \mathrm{i}} \log\left(\frac{\omega(\zeta, \alpha_\Gamma)}{|\alpha_\Gamma|\omega(\zeta, q^2/\overline{\alpha}_\Gamma)}\right) - \frac{\Gamma}{2\pi \mathrm{i}} \log\left(\frac{\omega(\zeta, 1)}{\omega(\zeta, q^2)}\right). \end{aligned} \tag{5}$$

2. Contribution from vortex shedding: $W_\kappa(\zeta)$

Using Eq. (4b), the complex potential induced by N shed vortices of strength κ_n at α_n, which have $-\kappa$ circulation around the plate C_1, is given by

$$\begin{aligned} W_\kappa(\zeta) &= \sum_{n=1}^{N} \kappa_n G^{(1)}(\zeta, \alpha_n) \\ &= \frac{1}{2\pi \mathrm{i}} \sum_{n=1}^{N} \kappa_n \log\left(\frac{\omega(\zeta, \alpha_n)}{|\alpha_n|\omega(\zeta, q^2/\overline{\alpha}_n)}\right), \end{aligned} \tag{6}$$

where $\kappa = \sum_{n=1}^{N} \kappa_n$.

3. Contribution from uniform flow: $W_U(\zeta)$

The complex potential induced by a uniform flow of magnitude 1 far upstream which produces no circulation around the plate is given by

$$W_U(\zeta) = -a\frac{\omega_\alpha(\zeta, 1)}{\omega(\zeta, 1)}. \tag{7}$$

where $\omega_\alpha(\zeta, 1)$ is the first derivative of $\omega(\zeta, 1)$ with respect to α and a is a constant such that

$$z \sim \frac{a}{\zeta - 1},$$

as $\zeta \to 1$. Expanding (1) in its Laurent series yields

$$a = A\,\omega(1, \mathrm{e}^{2\mathrm{i}\theta}).$$

4. Total complex potential

In summary, the total complex potential for a flat plate in ground effect with N shed vortices of strength κ_n located at α_n and an incident vortex of strength Γ located at α_Γ around the flat plate is given by

$$\begin{aligned} W \equiv \phi + \mathrm{i}\psi &= W_\Gamma(\zeta) + W_\kappa(\zeta) + W_U(\zeta) \\ &= \frac{\Gamma}{2\pi\mathrm{i}} \log\left(\frac{\omega(\zeta,\alpha_\Gamma)}{|\alpha_\Gamma|\omega(\zeta,q^2/\overline{\alpha}_\Gamma)}\right) - \frac{\Gamma}{2\pi\mathrm{i}} \log\left(\frac{\omega(\zeta,1)}{\omega(\zeta,q^2)}\right) \\ &+ \frac{1}{2\pi\mathrm{i}} \sum_{n=1}^{N} \kappa_n \log\left(\frac{\omega(\zeta,\alpha_n)}{|\alpha_n|\omega(\zeta,q^2/\overline{\alpha}_n)}\right) - a\frac{\omega_\alpha(\zeta,1)}{\omega(\zeta,1)}. \end{aligned}$$

The complex velocity field induced by this configuration of vortices may be calculated by differentiating the above, which yields

$$\begin{aligned} \frac{\mathrm{d}W}{\mathrm{d}\zeta} &= U(\zeta) - \mathrm{i}V(\zeta) \\ &= \Gamma G^{(1)}_\zeta(\zeta,\alpha_\Gamma) - \Gamma G^{(1)}_\zeta(\zeta,1) + \sum_{n=1}^{N-1}\left(\kappa_n G^{(1)}_\zeta(\zeta,\alpha_n) + \kappa_N G^{(1)}_\zeta(\zeta,\alpha_N)\right) + \frac{\mathrm{d}W_U}{\mathrm{d}\zeta}(\zeta). \end{aligned} \tag{8}$$

In terms of the Schottky-Klein prime function (3), the complex velocity is

$$\begin{aligned} \frac{\mathrm{d}W}{\mathrm{d}\zeta}(\zeta) = U(\zeta) - \mathrm{i}V(\zeta) = &\frac{\Gamma}{2\pi\mathrm{i}}\left(\frac{\omega_\zeta(\zeta,\alpha_\Gamma)}{\omega(\zeta,\alpha_\Gamma)} - \frac{\omega_\zeta(\zeta,q^2/\overline{\alpha}_\Gamma)}{\omega(\zeta,q^2/\overline{\alpha}_\Gamma)}\right) \\ &- \frac{\Gamma}{2\pi\mathrm{i}}\left(\frac{\omega_\zeta(\zeta,1)}{\omega(\zeta,1)} - \frac{\omega_\zeta(\zeta,q^2)}{\omega(\zeta,q^2)}\right) \\ &+ \frac{1}{2\pi\mathrm{i}}\sum_{n=0}^{N-1}\kappa_n\left(\frac{\omega_\zeta(\zeta,\alpha_n)}{\omega(\zeta,\alpha_n)} - \frac{\omega_\zeta(\zeta,q^2/\overline{\alpha}_n)}{\omega(\zeta,q^2/\overline{\alpha}_n)}\right) \\ &+ \frac{\kappa_N}{2\pi\mathrm{i}}\left(\frac{\omega_\zeta(\zeta,\alpha_N)}{\omega(\zeta,\alpha_N)} - \frac{\omega_\zeta(\zeta,q^2/\overline{\alpha}_N)}{\omega(\zeta,q^2/\overline{\alpha}_N)}\right) \\ &- a\left(\frac{\omega_{\alpha,\zeta}(\zeta,1)}{\omega(\zeta,1)} - \frac{\omega_\alpha(\zeta,1)\omega_\zeta(\zeta,1)}{\omega^2(\zeta,1)}\right), \end{aligned}$$

where κ_N is the circulation of the shedding vortex, and κ_n ($n = 1, 2, \cdots, N-1$) are the circulations of the free vortices which have been shed from the trailing edge of the plate.

The Kutta condition states that the velocity at the trailing edge of the plate is finite. Accordingly, W must vanish at $\zeta = \zeta_t$, where ζ_t is the location of the trailing edge of the plate in $\zeta-$space. Therefore, the instantaneous circulation of the shedding vortex κ_N is

$$\kappa_N = -\left[\Gamma G^{(1)}_\zeta(\zeta_t,\alpha_\Gamma) - \Gamma G^{(1)}_\zeta(\zeta_t,1) + \sum_{n=1}^{N-1}\kappa_n G^{(1)_\zeta}(\zeta_t,\alpha_n) + B\right] \Big/ G^{(1)}_\zeta(\zeta_t,\alpha_N), \tag{9}$$

where B is defined as

$$B = \frac{\mathrm{d}W_U}{\mathrm{d}\zeta}(\zeta_t) = -a\left(\frac{\omega_{\alpha,\zeta}(\zeta_t,1)}{\omega(\zeta_t,1)} - \frac{\omega_\alpha(\zeta_t,1)\omega_\zeta(\zeta_t,1)}{\omega^2(\zeta_t,1)}\right). \tag{10}$$

We note that the derivatives of the hydrodynamic Green's function are expressible in terms of the Schottky-Klein prime function (3) as

$$\begin{aligned} G^{(1)}_\zeta(\zeta,\alpha) &= \frac{1}{2\pi\mathrm{i}}\left(\frac{\omega_\zeta(\zeta,\alpha)}{\omega(\zeta,\alpha)} - \frac{\omega_\zeta(\zeta,q^2/\overline{\alpha})}{\omega(\zeta,q^2/\overline{\alpha})}\right), \\ G^{(1)}_{\zeta,\alpha}(\zeta,\alpha) &= \frac{1}{2\pi\mathrm{i}}\left(\frac{\omega_{\alpha,\zeta}(\zeta,\alpha)\omega(\zeta,\alpha) - \omega_\zeta(\zeta,\alpha)\omega_\alpha(\zeta,\alpha)}{\omega^2(\zeta,\alpha)}\right). \end{aligned}$$

The derivative of κ_N with respect to time t is given by

$$\frac{\mathrm{d}\kappa_N}{\mathrm{d}t} = -\frac{\Gamma G^{(1)}_{\zeta,\alpha}(\zeta_t,\alpha_\Gamma)}{G^{(1)}_{\zeta}(\zeta_t,\alpha_N)}\cdot\frac{\mathrm{d}\alpha_\Gamma}{\mathrm{d}t} - \frac{1}{G^{(1)}_{\zeta}(\zeta_t,\alpha_N)}\sum_{n=1}^{N-1}\kappa_n G^{(1)}_{\zeta,\alpha}(\zeta_t,\alpha_n)\cdot\frac{\mathrm{d}\alpha_n}{\mathrm{d}t}$$
$$+\frac{G^{(1)}_{\zeta,\alpha}(\zeta_t,\alpha_N)\left[\Gamma G^{(1)}_{\zeta}(\zeta_t,\alpha_\Gamma) - \Gamma G^{(1)}_{\zeta}(\zeta_t,1) + \sum_{n=1}^{N-1}\kappa_n G^{(1)}_{\zeta}(\zeta_t,\alpha_n) + B\right]}{\left(G^{(1)}_{\zeta}(\zeta_t,\alpha_N)\right)^2}\cdot\frac{\mathrm{d}\alpha_N}{\mathrm{d}t}.$$

C. Evolution of vortex shedding

The motion of the most recent vortex shed from the trailing edge is determined by the Brown and Michael equation [14],

$$\frac{\mathrm{d}\boldsymbol{x}_N}{\mathrm{d}t} + \frac{\boldsymbol{x}_N}{\kappa_N}\frac{\mathrm{d}\kappa_N}{\mathrm{d}t} = \boldsymbol{v}_N, \tag{11}$$

where $\boldsymbol{x}_N$ represents the location of a shed vortex tethered to the trailing edge with circulation κ_N in a vector form with respect to the rectangular coordinate system $\boldsymbol{x} \equiv (x, y)$, $\boldsymbol{v}_N$ is the fluid velocity at the location of $\boldsymbol{z}_N$ in a vector form when its local self-induced velocity contribution is excluded $\boldsymbol{v}_N \equiv (u, v)$. The Brown and Michael equation (11) governs the motion of the trailing-edge vortex until $\frac{\mathrm{d}\kappa_N}{\mathrm{d}t} = 0$. At this instant the circulation of the Brown-Michael vortex is fixed, the vortex is released into the wake as a free vortex, and a new Brown-Michael vortex is created at the trailing edge.

Equation (11) can be rewritten in a scalar form:

$$\frac{\mathrm{d}\alpha_N}{\mathrm{d}t} + \frac{1}{f'(\alpha_N)}\frac{f(\alpha_N) - f(\alpha_t)}{\kappa_N}\frac{\mathrm{d}\kappa_N}{\mathrm{d}t} = \frac{v^*_N}{f'(\alpha_N)}, \tag{12}$$

where α_N and α_t are the mapped vortex location of $z_N = x + \mathrm{i}y$ and the trailing-edge location in ζ-plane, respectively and

$$v^*_N = \left[\frac{1}{f'(\alpha_N)}\left(\frac{\mathrm{i}\kappa_N}{4\pi}\frac{f''(\alpha_N)}{f'(\alpha_N)} + F'(\alpha_N)\right)\right]^*, \tag{13}$$

The desingularised velocity field is represented by

$$F'(\alpha_N) = \lim_{\zeta\to\alpha_N}\left[\frac{\mathrm{d}W}{\mathrm{d}\zeta}(\zeta) - \frac{1}{2\pi\mathrm{i}}\frac{\kappa_N}{\zeta - \alpha_N}\right]. \tag{14}$$

Similarly, the motion for the incident vortex is governed by

$$\frac{\mathrm{d}\alpha_\Gamma}{\mathrm{d}t} = \frac{\left[\left(\frac{\mathrm{i}\Gamma}{4\pi}\frac{f''(\alpha_\Gamma)}{f'(\alpha_\Gamma)} + F'(\alpha_\Gamma)\right)\right]^*}{|f'(\alpha_\Gamma)|^2}, \tag{15}$$

where

$$F'(\alpha_\Gamma) = \lim_{\zeta\to\alpha_\Gamma}\left[\frac{\mathrm{d}W}{\mathrm{d}\zeta}(\zeta) - \frac{1}{2\pi\mathrm{i}}\frac{\Gamma}{\zeta - \alpha_\Gamma}\right]. \tag{16}$$

Finally, the motions for the $N-1$ "frozen" trailing edge vortices follow a similar form

$$\frac{\mathrm{d}\alpha_n}{\mathrm{d}t} = \frac{\left[\left(\frac{\mathrm{i}\kappa_n}{4\pi}\frac{f''(\alpha_n)}{f'(\alpha_n)} + F'(\alpha_n)\right)\right]^*}{|f'(\alpha_n)|^2}, \tag{17}$$

with

$$F'(\alpha_n) = \lim_{\zeta\to\alpha_n}\left[\frac{\mathrm{d}W}{\mathrm{d}\zeta}(\zeta) - \frac{1}{2\pi\mathrm{i}}\frac{\Gamma}{\zeta - \alpha_n}\right], \qquad \text{for } n = 1\,, 2\,, \cdots, N-1. \tag{18}$$

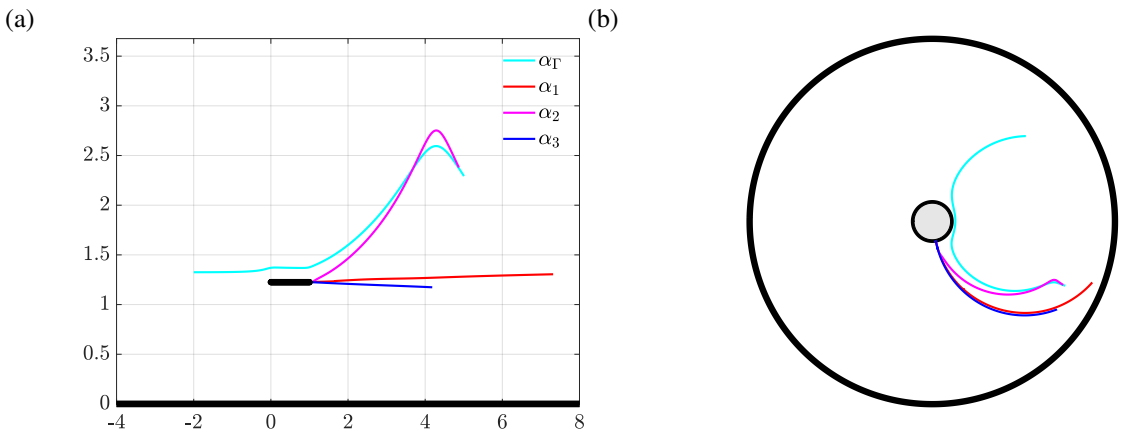

Fig. 3 Trajectories of the incident vortex α_Γ, and three shed vortices α_1, α_2 and α_3 in physical z-plane and mapped ζ-plane. $\theta = 0°$.

III. Results

In this section we plot results to investigate the vortex shedding from the trailing edge with the ground effect. The numerical simulations are carried out and are parameterized uniformly as follows:

$$\overline{x} = 2x/c,\ \overline{y} = 2y/c,\ \overline{\Gamma} = \Gamma/(\pi U c),\ \overline{t} = 2Ut/c.$$

A. Zero inclination angle ($\theta = 0$)

We first consider the case when an incident vortex α_Γ starts at the height $\Delta\overline{h} = 0.2$ above the airfoil with constant strength $\overline{\Gamma} = 0.2$ and passes by a flat plate airfoil with zero inclination angle ($\theta = 0$) in ground effect. The incident vortex induces fluid loading on the airfoil thereby causing the shedding of vorticity at the trailing edge. The trajectories of the vortices in physical z-plane and mapped ζ-plane are shown in Fig. 3, and the streamline at $\overline{t} = 14.97$ is shown in Fig. 4. Our simulations indicate that only three vortices are shed during this vortex-airfoil interaction, and the results are similar to previous work [16, 23] in the absence of a ground plane. Notably, while the trajectories of α_1 and α_3 remain in the vicinity of the x-axis, the trajectory of α_2, having an opposite sign of circulation to α_Γ, follows the trajectory of the incident vortex.

Figure 5 compares the corresponding time histories of airfoil circulation against that in the case of a free airfoil (without ground effect). The ground effect causes higher fluctuation of the airfoil circulation during the time when the incident vortex passes by the leading edge and the trailing edge of the airfoil. The approximate passing times are marked in red in Fig. 5. Notably, when the third shed vortex starts to slightly moving downward (see the blue curve in Fig. 3 (a)), the ground effect quickens approach of the airfoil circulation to its asymptotic long-time value.

B. Small inclination angle ($\theta = -10°$)

We also consider the case when the airfoil has a pitched angle to the x-axis. The vortex trajectories in both z-plane and ζ-plane, and the streamlines at different points in time are given in Fig. 6, Fig. 7, Fig. 8, Fig. 9 and Fig. 10, respectively.

IV. Conclusion

This paper has considered the shedding of vorticity from a plate interacting with an incident vortex in ground effect. The model framework is built using the Schottky-Klein prime function and is solved as a potential-flow problem. The motion of the shedding vortices are determined by the Brown and Michael equation, and the Kutta condition is satisfied to guarantee the flow leaving the trailing edge smoothly. We compared the simulation results with ground effect against previous works by [16, 23] in which the ground the effect is not considered. We obtained similar results for the vortex trajectories, but observed the effect of ground in stabilizing the airfoil circulation.

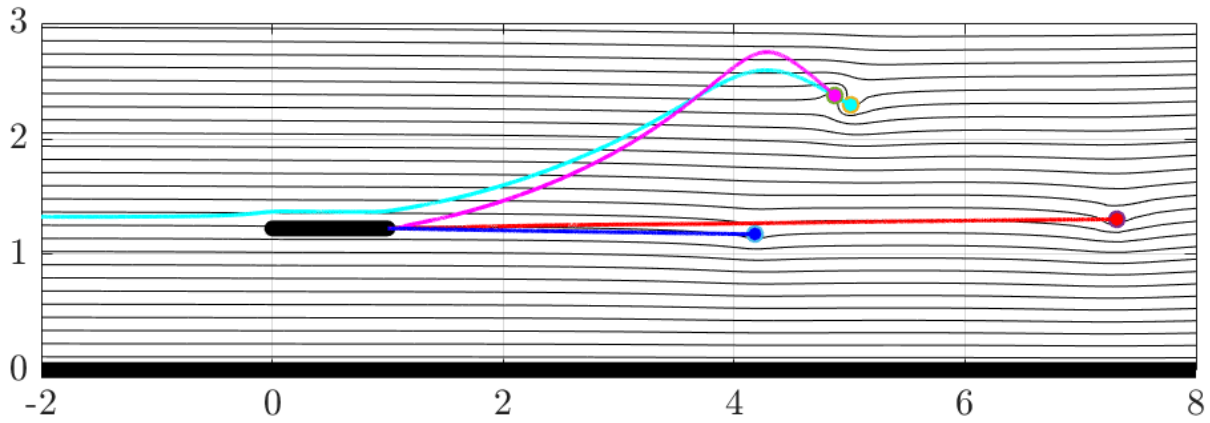

Fig. 4 The steady, uniform flow past a flat plate with zero inclination angle ($\theta = 0°$) in ground effect at $\bar{t} = 14.97$, with the Kutta condition specified. The instantaneous locations of the incident vortex and three vortices are marked as dots in cyan, red, magenta and blue. The corresponding previous vortex trajectories are marked in the same color as the dots.

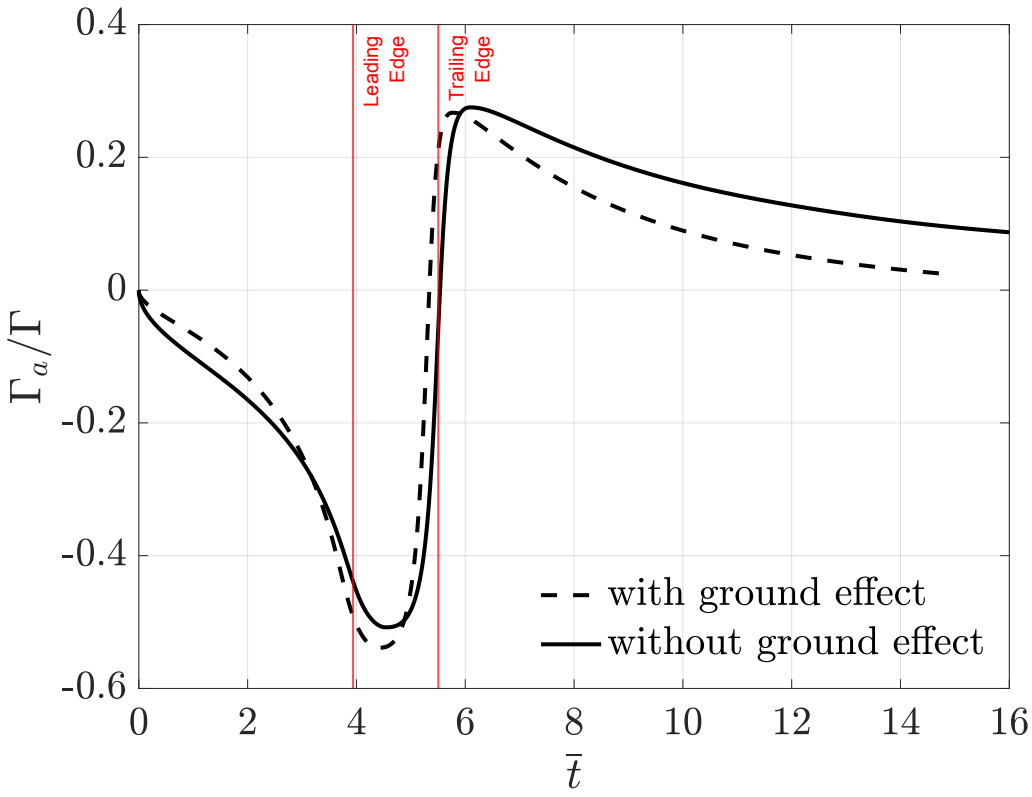

Fig. 5 Comparisons of airfoil circulation histories with and without ground effect. $\theta = 0°$.

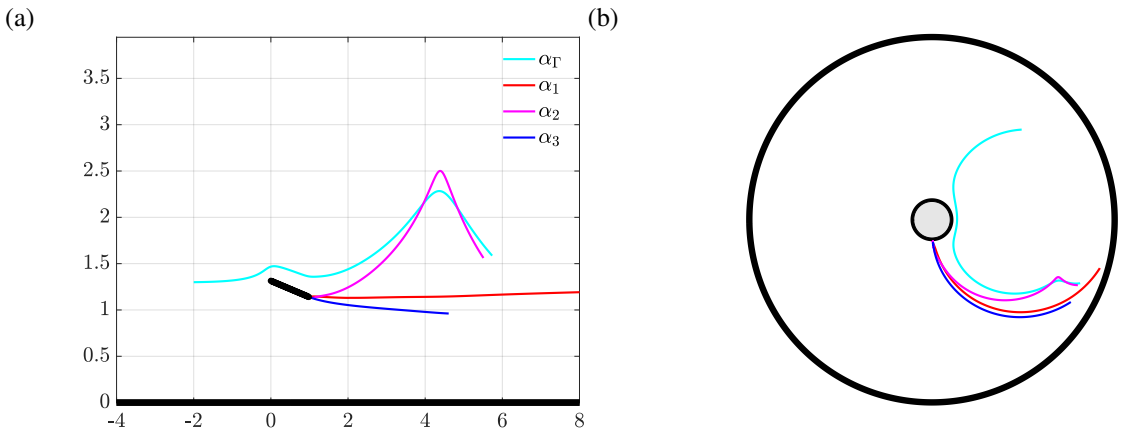

Fig. 6 Trajectories of the incident vortex α_Γ, and three shed vortices α_1, α_2 and α_3 in physical z-plane and mapped ζ-plane. $\theta = -10°$.

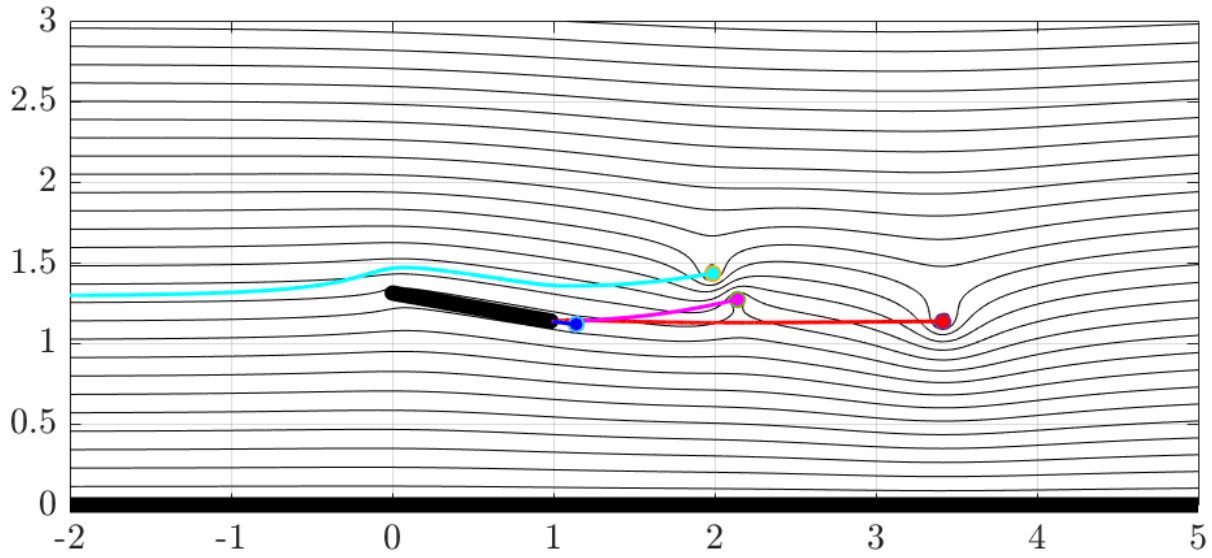

Fig. 7 The steady, uniform flow past a flat plate with inclination angle $\theta = -10°$ in ground effect at $\bar{t} = 6.37$, with the Kutta condition specified, for positive angle of attack. The instantaneous locations of the incident vortex and three vortices are marked as dots in cyan, red, magenta and blue. The corresponding previous vortex trajectories are marked in the same color as the dots.

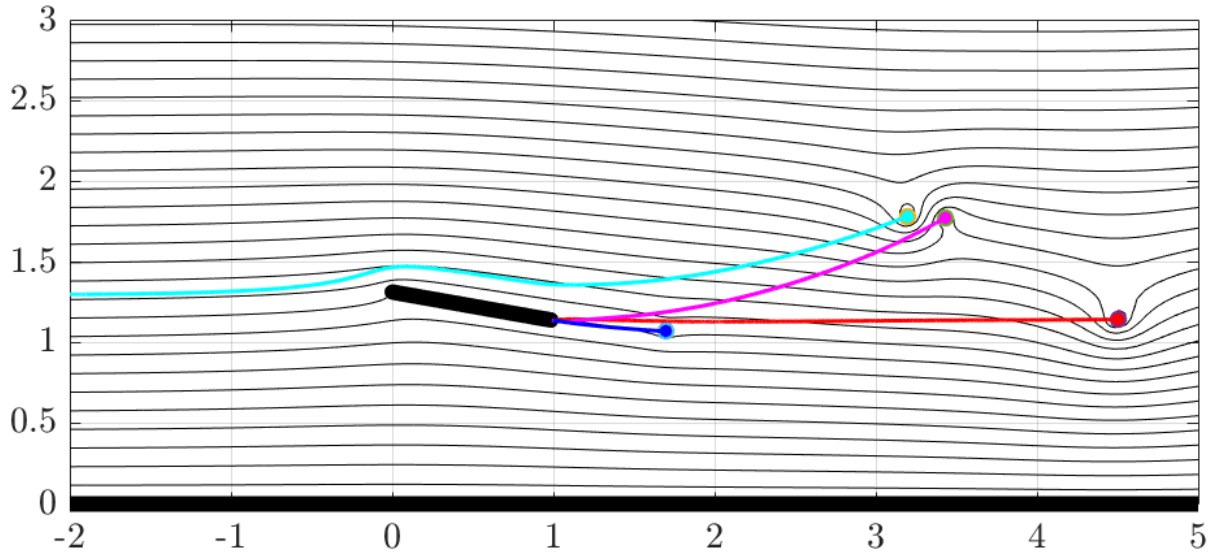

Fig. 8 The steady, uniform flow past a flat plate with inclination angle $\theta = -10^\circ$ in ground effect at $\bar{t} = 8.37$, with the Kutta condition specified, for positive angle of attack. The instantaneous locations of the incident vortex and three vortices are marked as dots in cyan, red, magenta and blue. The corresponding previous vortex trajectories are marked in the same color as the dots.

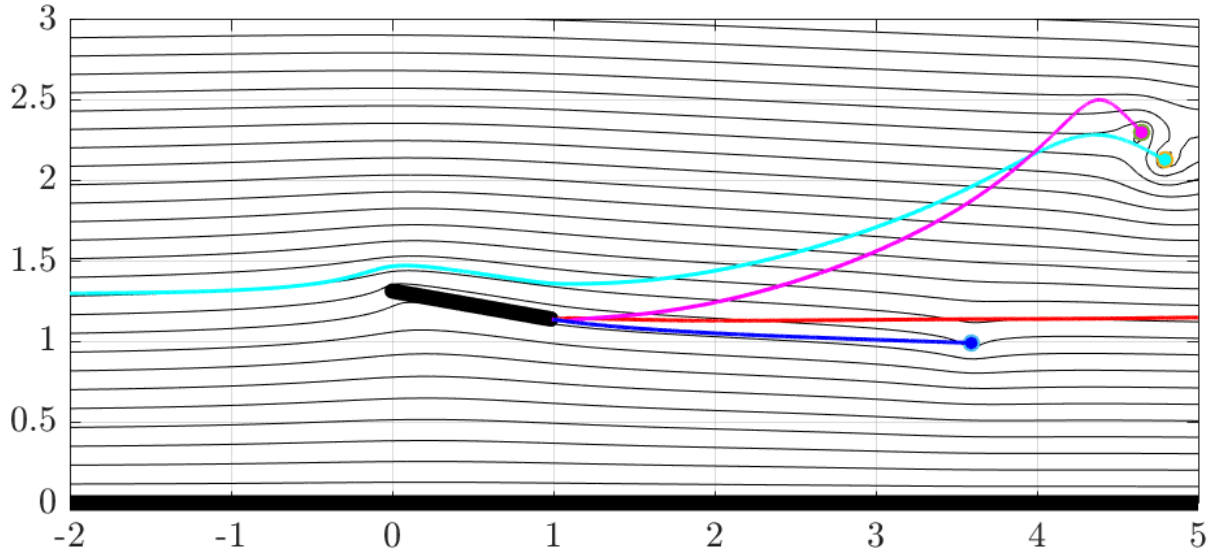

Fig. 9 The steady, uniform flow past a flat plate with inclination angle $\theta = -10^\circ$ in ground effect at $\bar{t} = 13.37$, with the Kutta condition specified, for positive angle of attack. The instantaneous locations of the incident vortex and three vortices are marked as dots in cyan, red, magenta and blue. The corresponding previous vortex trajectories are marked in the same color as the dots.

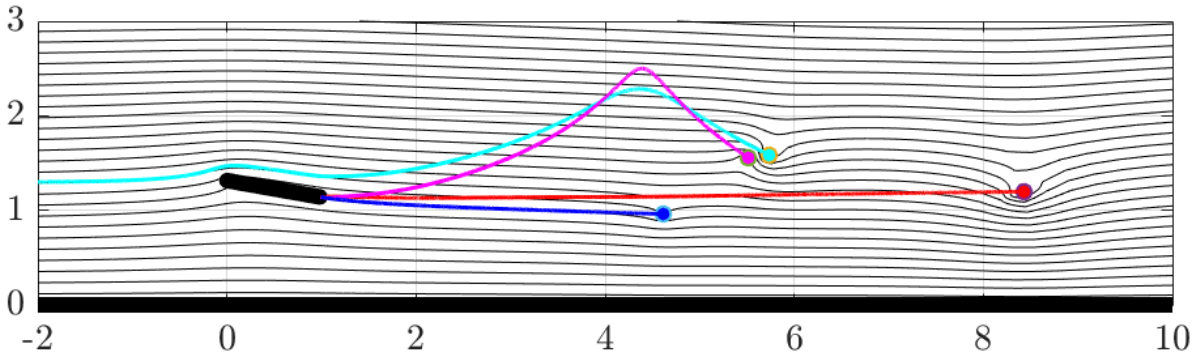

Fig. 10 The steady, uniform flow past a flat plate with inclination angle $\theta = -10^\circ$ in ground effect at $\bar{t} = 15.62$, with the Kutta condition specified, for positive angle of attack. The instantaneous locations of the incident vortex and three vortices are marked as dots in cyan, red, magenta and blue. The corresponding previous vortex trajectories are marked in the same color as the dots.

Future work will focus on the acoustic emissions of shed vortices in ground effect, which may be analysed using the compact Green's function for multiple bodies [24].

Acknowledgments

This work was supported in part by the Air Force Office of Scientific Research under AFOSR grant FA9550-15-1-0148, monitored by Drs. Douglas Smith and Gregg Abate, and by the National Science Foundation under awards 1805692 and 1846852, monitored by Dr. Ronald Joslin.

References

[1] Rayner, J. M. V., "On the Aerodynamics of Animal Flight in Ground Effect," *Philos. Trans. R. Soc. B Biol. Sci.*, Vol. 334, No. 1269, 1991, pp. 119–128. doi:10.1098/rstb.1991.0101.

[2] NATO RTO, "Fluid Dynamics Problems of Vehicles Operating Near or in the Air-Sea Interface," *RTO Appl. Veh. Technol. Panel Symp.*, 1998, p. 366.

[3] Holloran, M., and O'Meara, S., *Wing in Ground Effect Craft Review*, Melbourne, Australia, 1999.

[4] Rozhdestvensky, K. V., *Aerodynamics of a Lifting System in Extreme Ground Effect*, Springer, 2000. doi:10.1007/9783662042403.

[5] Michelin, S., and Llewellyn Smith, S. G., "An unsteady point vortex method for coupled fluid-solid problems," *Theor. Comput. Fluid Dyn.*, Vol. 23, No. 2, 2009, pp. 127–153. doi:10.1007/s00162-009-0096-7.

[6] Darakananda, D., and Eldredge, J. D., "A versatile taxonomy of low-dimensional vortex models for unsteady aerodynamics," *J. Fluid Mech.*, Vol. 858, 2019, pp. 917–948. doi:10.1017/jfm.2018.792.

[7] Abramowski, T., "Numerical investigation of airfoil in ground proximity," *J. Theor. Appl. Math.*, Vol. 45, No. 2, 2007, pp. 425–436.

[8] Willis, D., Peraire, J., and Breuer, K., "A Computational Investigation of Bio-Inspired Formation Flight and Ground Effect," *25th AIAA Appl. Aerodyn. Conf.*, American Institute of Aeronautics and Astronautics, Reston, Virigina, 2007, pp. 1–35. doi:10.2514/6.2007-4182.

[9] Quinn, D. B., Moored, K. W., Dewey, P. A., and Smits, A. J., "Unsteady propulsion near a solid boundary," *J. Fluid Mech.*, Vol. 742, 2014, pp. 152–170. doi:10.1017/jfm.2013.659.

[10] Widnall, S. E., and Barrows, T. M., "An analytic solution for two-and three-dimensional wings in ground effect," *J . Fluid Mech*, Vol. 41, No. 4, 1970, pp. 769–792. doi:10.1017/S0022112070000915.

[11] Iosilevskii, G., "Asymptotic theory of an oscillating wing section in weak ground effect," *Eur. J. Mech. - B/Fluids*, Vol. 27, No. 4, 2008, pp. 477–490. doi:10.1016/j.euromechflu.2007.08.005.

[12] Iosilevskii, G., "Indicial response functions in weak ground effect," *Eur. J. Mech. B/Fluids*, Vol. 33, 2012, pp. 40–57. doi:10.1016/j.euromechflu.2011.12.001.

[13] Brown, C. E., "Effect of leading-edge separation on the lift of a delta wing," *Journal of the Aeronautical Sciences*, Vol. 21, No. 10, 1954, pp. 690–694.

[14] Howe, M. S., "Emendation of the Brown & Michael equation, with application to sound generation by vortex motion near a half-plane," *Journal of Fluid Mechanics*, Vol. 329, 1996, pp. 89–101.

[15] Manela, A., and Huang, L., "Point vortex model for prediction of sound generated by a wing with flap interacting with a passing vortex," *The Journal of the Acoustical Society of America*, Vol. 133, No. 4, 2013, pp. 1934–1944.

[16] Chen, H., and Jaworski, J., "Vortex interactions with Joukowski airfoil on elastic supports," *2018 Fluid Dynamics Conference*, 2018. AIAA Paper 2907.

[17] Crowdy, D., and Marshall, J., "Conformal mappings between canonical multiply connected domains," *Comput. Methods Funct. Theory*, Vol. 6, No. 1, 2006, pp. 59–76. doi:10.1007/BF03321118.

[18] Crowdy, D., "Analytical formulae for source and sink flows in multiply connected domains," *Theor. Comput. Fluid Dyn.*, Vol. 27, No. 1-2, 2013, pp. 1–19. doi:10.1007/s00162-012-0258-x.

[19] Crowdy, D. G., Kropf, E. H., Green, C. C., and Nasser, M. M. S., "The Schottky-Klein prime function: A theoretical and computational tool for applications," *IMA J. Appl. Math.*, Vol. 81, No. 3, 2016, pp. 589–628. doi:10.1093/imamat/hxw028.

[20] Baddoo, P. J., and Ayton, L. J., "Vortex equilibria in ground effect," *2018 Fluid Dyn. Conf. AIAA Aviat. Forum*, American Institute of Aeronautics and Astronautics, Atlanta, Georgia, 2018, p. 2903. doi:10.2514/6.2018-2903.

[21] Crowdy, D., "A new calculus for two-dimensional vortex dynamics," *Theor. Comput. Fluid Dyn.*, Vol. 24, No. 1-4, 2010, pp. 9–24. doi:10.1007/s00162-009-0098-5.

[22] Crowdy, D., "Calculating the lift on a finite stack of cylindrical aerofoils," *Proceedings of the Royal Society A: Mathematical, Physical and Engineering Sciences*, Vol. 462, No. 2069, 2006, pp. 1387–1407.

[23] Manela, A., "Nonlinear effects of flow unsteadiness on the acoustic radiation of a heaving airfoil," *Journal of Sound and Vibration*, Vol. 332, No. 26, 2013, pp. 7076–7088.

[24] Baddoo, P. J., and Ayton, J. L., "The compact Green's function for multiple bodies," *25th AIAA/CEAS Aeroacoustics Conference*, 2019.